Angular effects in digital off-axis holography

Guojun Lai (赖国俊)[1], Gongxin Shen (申功炘)[1*], and Reinhard Geisler[2]

[1] *Institute of Fluid Mechanics, School of Aeronautic Science and Engineering, Beijing University of Aeronautics and Astronautics, Beijing 100191, China*

[2] *Institute of Aerodynamics and Flow Technology, German Aerospace Center, Bunsenstrasse 10, 37073 Göttingen, Germany*

[*] *E-mail: gx_shen05@yahoo.com.cn*

Received June 4, 2009

The relationship between the off-axis angle of the recording setup and the quality of reconstructed particle images in digital off-axis holography is studied. The interference patterns of the same particles in the same plane are recorded at different off-axis angles in horizontal and vertical directions. By means of numerical wave propagation, the particle images are reconstructed so as to evaluate and compare their quality by the numbers of particles picked out and by the signal-to-noise ratio (SNR). The results provide useful information about the relationship between the off-axis angle and the quality of the reconstructed image.

OCIS codes: 090.0090, 110.0110, 290.0290.

doi: 10.3788/COL20090712.1126.

In the early 1990s, when charged-coupled device (CCD) and highly capable computers became available[1], digital cameras have been directly used to record holograms. In recent years, efforts have been made to employ digital holography in experimental fluid dynamics to acquire three-dimensional (3D) particle images for further particle image velocimetry (PIV) processing. Many studies focus on how to improve the depth resolution (also called axial resolution) of digital reconstruction, in other words, to reduce the depth-of-focus (DOF) of the reconstructed particles[2−6]. In these researches, in-line holographic geometry is often adopted in hologram recording because the optical setup is simple. Recently, a type of digital holographic microscopy (DHM) setup, modified from a Mach-Zehnder interferometer, has been applied to digital holographic PIV[5,7]. This kind of off-axis holographic geometry seems to have had an influence on particle reconstruction because it involves off-axis angles in the digital recording[7]. However, few investigations have concerned themselves with its potential shortcoming. In this letter, we discuss the relationship between off-axis angle of the recording setup and quality of the reconstructed particle images. In the experiment, we adopt the digital reconstructing method presented by Colomb *et al.*[8,9] to extract the amplitude information of particles from digital holograms. The fringes of the same particles on the same plane are recorded at different off-axis angles.

As is known, in a full-frame interline transfer CCD, the vertical shift registers located between active pixels are masked. Considering the non-isotropic geometrical layout of a single pixel, holograms are recorded at horizontal and vertical off-axis angles. Then, particle images are reconstructed numerically so as to evaluate and compare their quality by particle numbers picked out from the reconstructed images and average signal-to-noise ratio (SNR) of the particles. The results provide useful information with respect to the relationship between the off-axis angle and the quality of the reconstructed image, taking into account the anisotropic geometry of the pixels.

The intensity of a hologram which comes from the interference between the reference wave R and the object wave O is

$$I_{\mathrm{H}} = (R+O)(R+O)^* = |R|^2 + |O|^2 + R^*O + RO^*. \quad (1)$$

The first two terms and the last term (i.e., the zeroth order diffraction and the real image) can be eliminated numerically by means of filtering their spatial frequencies in the spectrum of hologram[10,11]. Then, we have a new hologram

$$I'_{\mathrm{H}} = R^*O. \quad (2)$$

There is no doubt that I'_H is a complex function and only the information of the virtual image is left in this new hologram.

The wavefront of the virtual image $\Gamma(\xi,\eta)$, including the amplitude and phase distribution, can be obtained by calculating the Fresnel-Kirchhoff integral,

$$\Gamma(\xi,\eta) = \frac{1}{\mathrm{i}\lambda d}\exp(\mathrm{i}\frac{2\pi}{\lambda}d)\exp\left[\mathrm{i}\frac{\pi}{\lambda d}(\xi^2+\eta^2)\right] \times \iint R_{\mathrm{D}}(x,y)I'_{\mathrm{H}}(x,y)\exp\left[\mathrm{i}\frac{\pi}{\lambda d}(x^2+y^2)\right] \times\exp\left[-\mathrm{i}\frac{2\pi}{\lambda d}(x\xi+y\eta)\right]\mathrm{d}x\mathrm{d}y, \quad (3)$$

where λ is the wavelength, d is the reconstructing distance, I'_{H} is the filtered hologram, $R_{\mathrm{D}}(x,y)$ is the digital reference wave[12]. It should be noticed that the Fresnel approximation is valid only if the following inequality is fulfilled[13]:

$$d^3 \gg \frac{\pi}{4\lambda}\left[(\xi-x)^2+(\eta-y)^2\right]^2_{\max}. \quad (4)$$

Considering this off-axis optical geometry, it is also noticed that the off-axis angle between the reference beam and the object beam is limited by the pixel size Δw of the CCD and the wavelength λ of the laser according to

the Nyquist-Shannon theorem. The maximum angle can be calculated with[13]

$$\theta_{\max} \approx \frac{\lambda}{2\Delta w}. \quad (5)$$

If we substitute Δw with 6.45 μm and λ with 632.8 nm (a He-Ne laser), we obtain the maximum off-axis angle allowed in this experiment is about 2.8°. If the off-axis angle is larger than 2.8°, aliasing will occur and the resultant spatial image frequencies will influence the reconstruction. However, the intensity of the interference pattern is integrated over the finite area of the single pixels, which acts as a low-pass filter. As a result, the image frequencies will be dampened. In addition, the information of a single particle position is distributed over a certain range of spatial frequencies depending on the position on the CCD sensor. As a consequence, reconstruction of the particles will still be possible at high off-axis angles, even though the reconstruction quality will change. This influence is investigated in this letter.

As introduced by Colomb *et al.*[8], Eq. (3) can be digitized in two different numerical formulations, i.e., the Fourier transform formulation and the convolution formulation. In this experiment, the convolution formulation is utilized to reconstruct the wavefront at a series of planes along the depth direction. Another special algorithm, presented by Colomb *et al.*[9], is applied to compensate for the aberration of the wavefront including the tilt caused by the off-axis geometry. In this algorithm, compensation can be achieved just by multiplying the filtered hologram by the conjugated phase of a reference hologram which is recorded without any specimen in the object arm[9].

The experimental setup, presented in Fig. 1, is modified from a Mach-Zehnder interferometer. Digital holograms are recorded by a cooled digital 12-bit CCD camera, the resolution of which is 1376×1040 pixels. The pixel size is 6.45 μm. A He-Ne laser is used as light source. A piece of slide glass on which opaque particles (5 μm in diameter) are homogeneously dispersed is placed perpendicular to the object beam as specimen. The reference beam and the object beam are assumed to propagate towards the CCD in the negative z direction. In order to adjust the off-axis angle between the reference beam and the object one, a mirror M2 is mounted on a rotation stage. As long as the mirror is rotated only a little, the reference beam will be still projected onto the CCD at the corresponding incident angle, i.e., off-axis angle.

We establish a coordinate frame on the CCD as shown in Fig. 2 and assume that the reference beam propagates in the negative z direction. The incident angle is defined as the acute angle between the wave vector of the reference beam and the z axis. In this experiment, if the incident plane of the beam is the y-z plane, the incident angle is defined as the vertical off-axis angle or the vertical incident angle (i.e., angle β in the diagram). Likewise, if the incident plane of the beam is the x-z plane, the incident angle is defined as the horizontal off-axis angle or the horizontal incident angle (i.e., angle α in the diagram). Digital holograms are all recorded with the reference beam projected on the chip either at a horizontal or vertical incident angle.

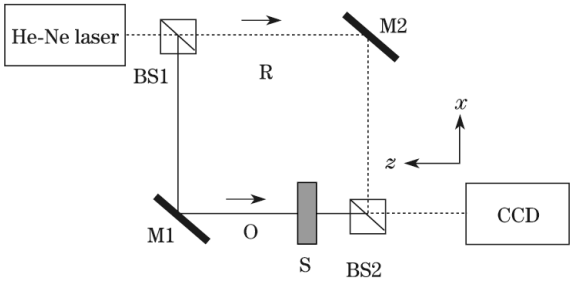

Fig. 1. Experimental setup. BS1 and BS2 are beam splitters, M1 and M2 are mirrors, O and R represent the object wave and the reference wave, respectively, S is the experiment specimen, a piece of slide glass with particles.

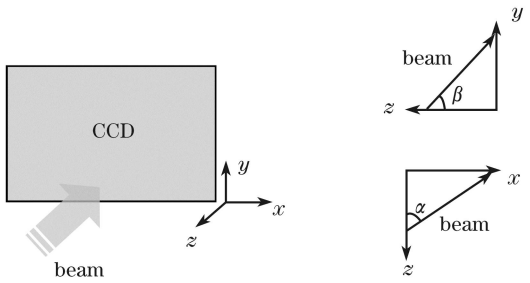

Fig. 2. Geometric diagram of the beam and the CCD.

The experimental specimen, a piece of slide glass with opaque particles being evenly dispersed, is placed perpendicular to the object beam as shown in Fig. 1. Digital holograms are recorded in the off-axis holographic geometry (Fig. 2) at two different recording distances, 221.4 and 212 mm. In order to investigate the relationship between the off-axis angle of the recording setup and the quality of reconstructed particle images, the incident angle of the reference beam, i.e., the off-axis angle in the holographic geometry, is adjusted from 1.6° to 5.2° by 0.2° steps. On one hand, 1.6° is the minimum off-axis angle at which the carrier frequencies of real image and those of virtual image do not overlap in the spectrum of the holograms (Fig. 3(a)) in this experiment. On the other hand, the angle cannot be more than 5.2° due to the CCD size and the overlapping of frequency components in the spectrum, as presented in Fig. 3(b). Apparently, this maximum off-axis angle is almost twice the theoretical maximum off-axis angle according to Eq. (5), with the consequences mentioned above.

It is known that there is an inherent problem associated with interline-transfer-CCDs. In the geometrical layout of the image pixels on the CCD (Fig. 4), the masked vertical shift registers are located between the active pixels. In other words, they are light insensitive and make the light sensitive area of a single pixel rectangular. In order to increase the sensitivity to incident light, micro lenses are placed over each pixel. However, the non-isotropic characteristic of the geometrical layout remains, which especially results in a different angular response of the CCD in the horizontal and the vertical directions. Thus holograms are recorded at horizontal and vertical off-axis angles, respectively, so as to ascertain which case the quality of reconstructing images is more sensitive to.

Particle images are reconstructed slice by slice in the

depth direction (i.e., z axis in Fig. 2) by calculating the Fresnel-Kirchhoff integral. The reconstructed step is 0.04 mm (i.e., the distance between two adjacent reconstructed images is 0.04 mm). The images are 512×512 pixels in size, as shown in Figs. 3(c) and (d).

Only the amplitude of the particle image is discussed and the phase information is excluded in the discussion. In the holographic PIV, only the amplitude of particle image concerns the researchers because it provides the information of the particle position which is valuable in velocity measurements. The phase does not nearly provide any information about the particle position. Therefore, the discussion on the phase is excluded in this letter.

In holographic PIV, the measurement must suffer from the so-called poor particle image DOF. The particle image DOF referred here means the depth length of reconstructed particle images. Due to the limited recording resolution of digital hologram and the image quality, the reconstructed particle image is not a sphere but cigar-like shape. It implies that the accuracy of depth position of those reconstructed particle images is poor. The position accuracy of the reconstructed particle images is very important to the holographic PIV because it directly influences the accuracy of further velocity evaluation by cross correlation of the two images captured at two consecutive exposures. In this experiment, all particles are dispersed on a plane, thus the variation of particle numbers on reconstructed planes in the depth direction can directly present the particle image DOF. Better particle image DOF must tell better image quality since the recording resolution of all holograms are the same. It should also be emphasized that all digital holograms have recorded exactly the same particles on that glass for a reasonable comparison. In the reconstructed particle images, particles are bright and the background is dark. Thus particles can be identified easily with the common "clean-algorithm". The procedure of this algorithm encompasses five steps: finding the maximum value of the gray scale image, calculating a Gaussian fit around that spot, subtracting the fitted surface from the image, finding the location of the next maximum, and redoing above four steps until the maximum gray intensity of this image is under a threshold value. In this experiment, the threshold of picking out the particles is defined as 0.65 in gray scale value (the range of gray scale values is from 0 to 1; 1 is white and 0 is black.). Then particles are identified and counted with the threshold value. The average diameter of the particles picked out from the images is about 6 pixels.

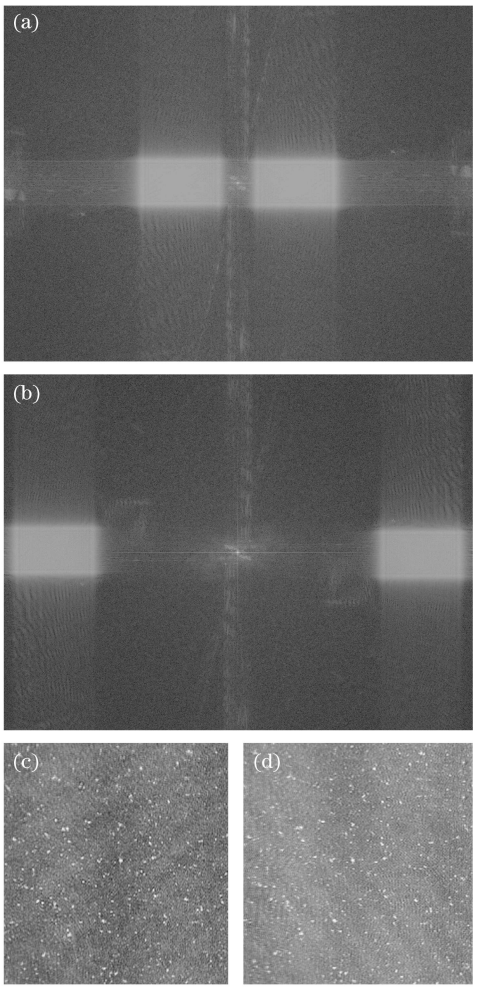

Fig. 3. Hologram spectra at (a) 1.6° and (b) 5.2° of off-axis angle. The gray square on the left holds the carrier frequencies of real image, the one on the right holds the carrier frequencies of virtual image, in the middle there is the direct current term. In (a), the carrier frequencies of real image and virtual image almost overlap. In (b), the frequency components may overlap with other periods. (c) and (d) present two reconstructed images. The recording distance is 212 mm. The off-axis angle is horizontal 2.8° for (c) and vertical 2.8° for (d).

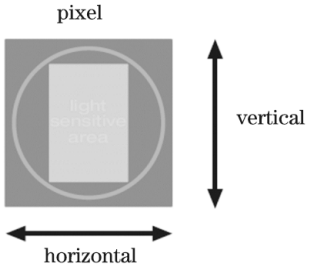

Fig. 4. A single image pixel with a typical relation between total size and light sensitive area (the rectangle area in the middle). The circle shows a potential micro-lens. (From the technical note of the PCO company, "Shading in cameras with large image sensors".)

In Fig. 5, the particle numbers of the reconstructed images along the z axis, normalized to the maximum particle number respectively, are demonstrated for each case of off-axis angles. Furthermore, they are averaged over all angles for each incident case (horizontal or vertical), as shown in Fig. 6. By comparison, it is found that the width of the peaks slightly broadens as the recording distance increases from 212 to 221.4 mm. This must be attributed to the increase of the particle image DOF because it would rise as the recording distance increases[14]. Therefore, when the recording distance increases from 212 to 221.4 mm, the particle image DOF must increase simultaneously. Specially, in this experiment, all particles were dispersed on a piece of glass (i.e., in one plane). If the particle image DOF of a reconstructed particle increases, the particle would appear in more consecutive reconstructed images. Thus, it

would raise the particle numbers and make the curves of the particle numbers versus the reconstructed distances broader. If these curves are broad, it can be inferred that the particle image DOF is large. To some extent, these curves "visualize" the particle image DOF.

It is also found in Figs. 6(a) and (b) that the width of the peak in the vertical case is a little boarder than the width in the horizontal case. Based on the connection between the particle image DOF and the curve shape, this leads to the conclusion that the particle image DOF for vertical incidence is longer. After all, the difference between the horizontal and vertical incidence cases is small in Fig. 6. Thus, based on the data obtained so far, it comes to a conclusion that the incident direction could influence the particle image DOF and the horizontal incidence provides a slightly better result.

As mentioned above, the "clean-algorithm" is used to pick out particles in the reconstructed images. At the same time, the average gray intensity of each particle is calculated and the residual image is utilized to calculate the standard deviation of the background noise after the out-of-focus particle images are eliminated by another "clean-algorithm" with a lower threshold value.

The average SNR of a particle is presented in Fig. 7. Obviously, the horizontal incidence of the reference beam leads to better SNR in contrast with the vertical incidence of the reference beam at the incident angle (i.e., off-axis angle) of the same degrees. Meanwhile, the average SNR tends to increase with an increase of the off-axis angle. Whereas, for vertical incidence, the average

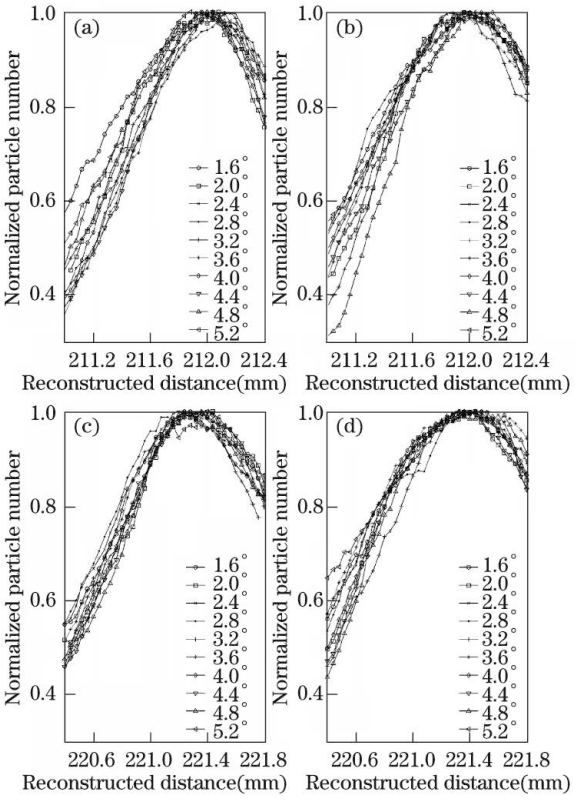

Fig. 5. Normalized particle number versus the reconstructed distance at different off-axis angles. The incident angles of the reference beam: (a) and (c) are horizontal; (b) and (d) are vertical. The recording distances of the holograms: (a), (b) 212 mm; (c), (d) 221.4 mm.

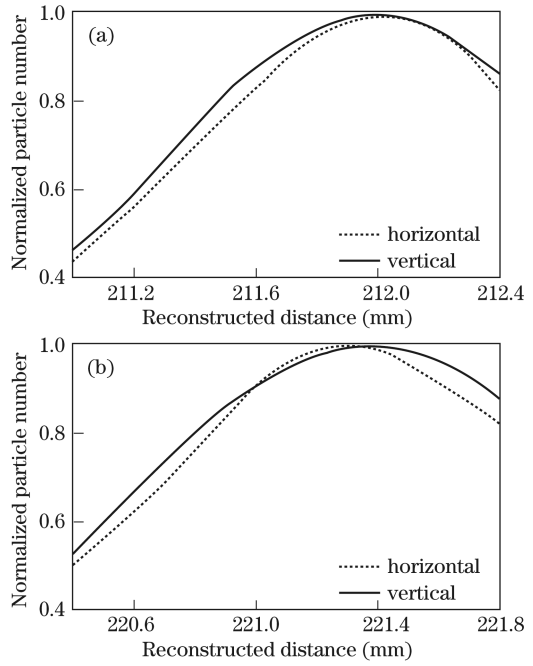

Fig. 6. Average normalized particle number over ten off-axis angles at recording distances of (a) 212 mm and (b) 221.4 mm.

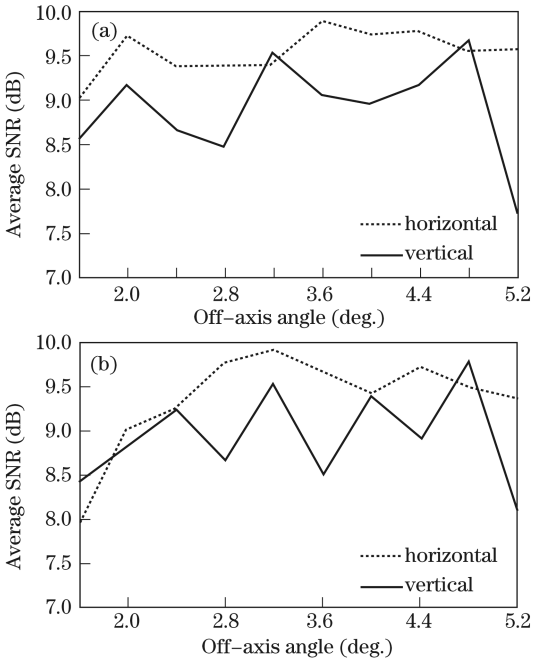

Fig. 7. Average SNR of particle at horizontal and vertical off-axis angles. The recording distances of the holograms are (a) 212 mm and (b) 221.4 mm.

SNR drops suddenly as the off-axis angle increases from 4.8° to 5.2°, in comparison, for the horizontal incidence, the average SNR remains almost the same.

In conclusion, we study the angular effects on the quality of the reconstructed images in digital off-axis holography. The particle number and the SNR of particles are used to evaluate the image quality. The incident direction of the reference beam influences the particle image DOF and the horizontal incidence provides slightly better particle image DOF. However, it requires further experiment

regarding the recording distance to find out the interaction between the incident direction of reference beam and the recording distance, which is known as an important factor that definitely plays a part in the depth resolution. The difference in SNR also suggests slightly better data quality in the case of horizontal incidence than in the case of vertical incidence. Reasonable explanation could be given if further knowledge of the exact geometry of the pixels and on-chip lenses are available. The important point in this study is the fact that the image quality is not very sensitive to the off-axis angle within the investigated range. Especially, the angular limit according to Eq. (5) derived from the Nyquist-Shannon theorem can be transcended without a significant drop in the image quality. Future work will lay emphasis on the interaction among factors like axial depth of fluid volume, pixel size, and off-axis angle, so as to determine the connection between the pixel size and the limitation of off-axis angle beyond the commonly used Eq. (5).

This work was supported by an AIRNET grant from Airbus, DLR's Institute of Aerodynamics and Flow Technology in Göttingen and the National Natural Science Foundation of China (No. 10772017).

References

1. U. Schnars and W. P. O. Jüptner, Meas. Sci. Technol. **13,** R85 (2002).
2. G. Pan and H. Meng, Appl. Opt. **42,** 827 (2003).
3. G. Shen and R. Wei, Opt. Lasers Eng. **43,** 1039 (2005).
4. T. Ooms, W. Koek, J. Braat, and J. Westerweel, Meas. Sci. Technol. **17,** 304 (2006).
5. J. Sheng, E. Malkiel, and J. Katz, Appl. Opt. **45,** 3893 (2006).
6. H. Wang, B. Zhao, and X. Song, Acta Opt. Sin. (in Chinese) **29,** 374 (2009).
7. L. Cao, G. Pan, S. H. Woodward, and H. Meng, "Hybrid digital holographic imaging system for 3D dense particle field measurement" presented at the *7th International Symposium on Particle Image Velocimetry* (2007).
8. T. Colomb, F. Montfort, J. Kuhn, N. Aspert, E. Cuche, A. Marian, F. Charrière, S. Bourquin, P. Marquet, and C. Depeursinge, J. Opt. Soc. Am. A **23,** 3177 (2006).
9. T. Colomb, J. K. Kühn, F. Charrière, C. Depeursinge, P. Marquet, and N. Aspert, Opt. Express **14,** 4300 (2006).
10. E. Cuche, P. Marquet, and C. Depeursinge, Appl. Opt. **39,** 4070 (2000).
11. W. Liu, Y. Dai, X. Kang, F. Yang, and X. He, Acta Opt. Sin. (in Chinese) **28,** 856 (2008).
12. E. Cuche, P. Marquet, and C. Depeursinge, Appl. Opt. **38,** 6994 (1999).
13. J. W. Goodman, *Introduction to Fourier Optics* (3rd edn.) (Roberts and Company Publisher, Englewood, 2005).
14. Y. Zhang, G. Shen, A. Schröder, and J. Kompenhans, Opt. Eng. **45,** 075801 (2006).